Int J Clin Exp Pathol 2021;14(4):408-416
www.ijcep.com /ISSN:1936-2625/IJCEP0121847

Original Article

Resiniferatoxin reduces cardiac sympathetic nerve activation to exert a cardioprotective effect during myocardial infarction

Ludefu Su, Yu Liu, Yanhong Tang, Mingmin Zhou, Liang Xiong, Congxin Huang

Department of Cardiology, Renmin Hospital of Wuhan University, Cardiovascular Research Institute of Wuhan University, Hubei Key Laboratory of Cardiology, Wuhan 430000, People's Republic of China

Received September 6, 2020; Accepted December 10, 2020; Epub April 15, 2021; Published April 30, 2021

Abstract: Background and objective: Myocardial infarction (MI) is a common critical disease of the cardiovascular system. The process of MI is often accompanied by the excessive activation of cardiac sympathetic nerves, which leads to arrhythmia. Resiniferatoxin (RTX) is a transient receptor potential vanilloid 1 (TRPV1), involved in the cardiac sympathetic afferent reflex. However, whether RTX can reduce the occurrence of arrhythmia and exert a cardioprotective effect by inhibiting the sympathetic reflex during MI is still unknown. Methods: The left anterior descending artery of cardiac was clamped to construct a model of MI. RTX (50 μg/ml) was used by epicardial application in MI rats. Ventricular electrophysiologic properties were continuously monitored by a body surface ECG. Yrosine hydroxylase (TH) and growth associated protein 43 (GAP43) were detected by Immunofluorescence staining. Connexin43 and transforming growth factor beta receptor 1 (TGF-β1) were detected by western blot. Norepinephrine (NE) and BNP levels in blood and tissue were determined by ELISA. Cardiac function was assessed by echocardiography. Results: The ERP, APD90, QRS, QT and the Tend-Tpeak intervals in MI rats were all prolonged, but decreased after RTX treatment (n = 3, P<0.05). In contrast, the RR interval was shortened in the MI group, but prolonged in the MI+RTX group (n = 3, P<0.05). RTX treatment significantly reduced ventricular arrhythmias after MI. TH- and GAP43-positive nerve densities and TGF-β1, and cx-43 protein expression were up-regulated in the MI group compared to the sham group, and they were decreased in the MI+RTX group compared to the MI group (n = 3, P<0.05). RTX can decrease serum and tissue NE and BNP levels (n = 3, P<0.05). RTX pretreatment significantly decreased heart rate, HW/BW ratio and LVIDS, and increased LVEF andLVFS values (n = 3, P<0.05). Conclusion: RTX improved cardiac dysfunction, ventricular electrophysiologic properties, and sympathetic nerve remodeling in rats with MI by inhibiting the excessive cardiac sympathetic drive.

Keywords: Cardiac sympathetic afferent reflex, myocardial infarction (MI), resiniferatoxin (RTX)

Introduction

Myocardial infarction (MI) is a common critical disease of the cardiovascular system with extremely high mortality and disability rates [1, 2]. Ventricular arrhythmias (VAs) after infarction, especially ventricular tachycardia and ventricular fibrillation, are the most important factors causing death and disability from MI [3]. Identifying the best prevention and treatment strategy for VAs after MI is a core issue in current clinical and basic research.

Related experiments have confirmed that excessive activation of cardiac sympathetic nerve input leads to local electrophysiological heterogeneity and a susceptibility to arrhythmia causing various types of VAs [4, 5]. At the same time, abnormally activated sympathetic nerves after an MI can release a large amount of norepinephrine (NE), which affects the peripheral cardiovascular system, leading to sharp increases in the heart rate and blood pressure, and further aggravating myocardial injury and compromising cardiac function [6-8]. Therefore, studying the regulation of cardiac sympathetic nerves can provide a solid theoretical basis for the prevention and treatment of arrhythmia after MI [9].

Resiniferatoxin (RTX) is a transient receptor potential vanilloid 1 (TRPV1) agonist isolated

from an ultrapotent capsaicin analog [10], which can irreversibly desensitiz TRPV1 expressed at the dorsal root ganglion (DRG) of neurons [11], involved in the cardiac sympathetic afferent reflex. In order to study the regulatory effect of epicardial application of RTX on CSAR in MI, and whether it exerted cardioprotective effects, RTX was applied to the epicardium during MI induction in rat models.

Materials and methods

Experimental animals

Male Sprague-Dawley (SD) rats (200-250 g) were provided by the Experimental Animal Center, and all experiments conformed to the guidelines for the Care and Use of Laboratory Animals published by the US National Institutes of Health (NIH Publication 85-23, revised 1996) and were approved by the Ethics Committee of Animal Care and Use Committee of Renmin Hospital of Wuhan University, China. The rats were divided into a sham group (n = 10), an MI group (n = 15), a sham+RTX group (n = 10), and an MI+RTX group (n = 15).

Rat myocardial infarction model and treatment

Briefly, the rats were anesthetized with 80 mg/kg pentobarbital sodium injected intraperitoneally, intubated, and connected to a rodent ventilator (respiratory ratio: 1:1.5, tidal volume: 3-4 ml/100 g). An 8-0 Prolene suture was used to ligate the left anterior descending artery. The ST segment of the ECG and regional cyanosis of the myocardial surface determined whether the myocardial infarction model was successfully constructed. RTX (50 μg/ml) was injected through epicardial application.

Measurements of ventricular electrophysiological properties in vivo

A body surface ECG was continuously monitored using the PowerLab Data Acquisition System. The heart was completely exposed. A custom-made Ag-AgCl electrode was used to record the monophasic action potential (MAP), and the action potential duration was determined at 90% repolarization (APD90) at three distinct recording sites within each ventricle to calculate the mean LV and right ventricular (RV) APD90 values. All MAP signals were recorded and analyzed using the PowerLab System (AD Instruments Ltd., Chalgrouve, UK) and Chart 7.0 software (AD Instruments) [12]. The duration of a persistent VA episode was greater than 2 seconds, whereas VA episodes lasting less than 2 seconds were considered non-sustained VA episodes [13].

Immunohistochemistry

The heart was removed and embedded in paraffin for immunohistochemistry. Immunoreactivity was expressed as the infarct border area of positive staining per square millimeter (mm^2). Immunofluorescence staining was used to evaluate sympathetic innervation of the infarct border area. Heart tissue was washed with PBS and stained with a rabbit polyclonal antibody against tyrosine hydroxylase (TH) and growth associated protein 43 (GAP43) diluted 1:1000. Primary antibody binding was detected using the Bond Polymer Refine Detection Kit (Leica, Wetzlar, Germany), then counterstained with hematoxylin, dehydrated and mounted. All slides were observed under a microscope [14].

Western blotting analysis

For western blot, samples were dissolved with Tris-HCl buffer and a mixture of proteinase and phosphatase inhibitors (Aspen, US). Transforming growth factor beta receptor 1 (TGF-β1) (1:1000 dilution, Abcam, US), and connexin 43 (1:3000, Abcam, US), followed by HRP-goat anti-rabbit secondary antibody (1:10000, Aspen, US). GAPDH (1:10000, Abcam, US) was used as a control to verify equal protein loading. The densitometric results for TGF-β1 and connexin 43 were reported as the ratios to GAPDH.

Serum and myocardial tissue NE and BNP levels

A total of 3-4 ml of peritoneal venous blood was collected into tubes containing 10 ml of EDTA, and the samples were immediately centrifuged for plasma separation. LV myocardial tissue (100-150 mg) was homogenized using a homogenizer to produce a 10% tissue homogenate. NE levels in serum and tissue were measured by an enzyme-linked immunosorbent assay kit (ELISA, Biolegend Inc.). Blood samples were collected from eye veins of four-week-old mice. NE levels in blood and tissue were determined by ELISA (Biolegend Inc.) according to

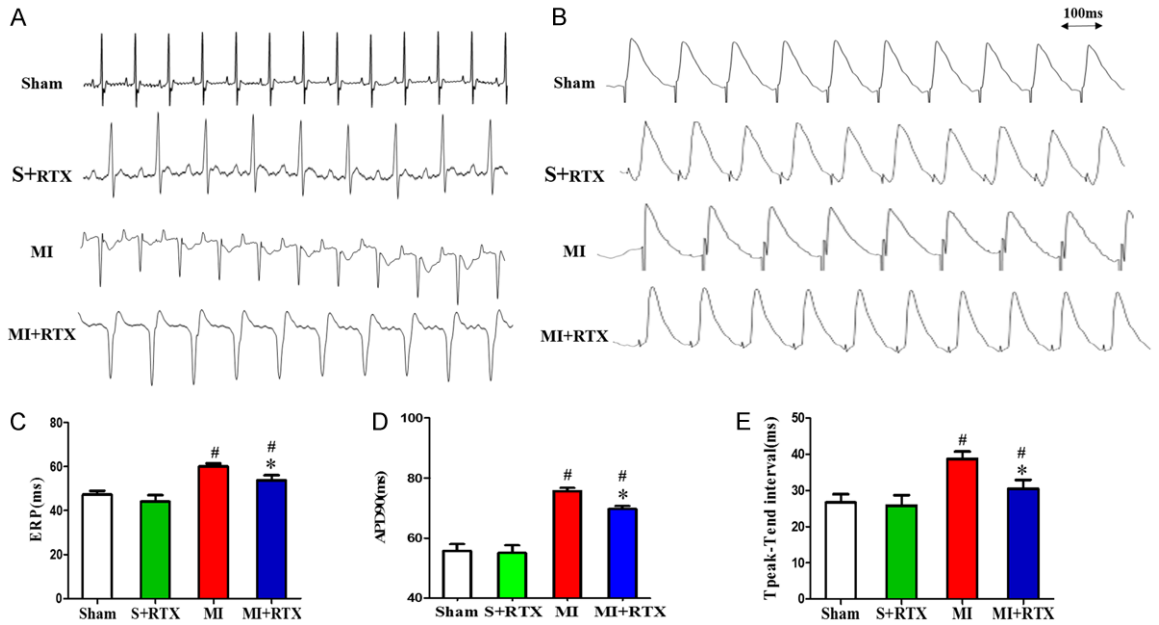

Figure 1. Effects of RTX on ventricular repolarization. A. Representative electrocardiogram. B. Representative APD recorded from the LV of each group. C. ERP (ms) in each group. D. APD90 (ms)in each group. E. Tpeak-Tend interval (ms) in each group. #*P*<0.05 versus Sham group. **P*<0.05 versus MI group. APD90 indicates action potential duration at 90% repolarization; LV, left ventricular; ERP: the ventricular effective refractory.

the recommendations of the manufacturer. The OD value at 450 nm was detected using a microplate reader (MQX 200, BioTek Instruments, Winooski, VT, USA).

Analysis of the echocardiographic values

Echocardiography analysis was performed using a high-resolution imaging system with a 30-MHz high-frequency scanhead (VisualSonics Vevo770, VisualSonics, Toronto, Canada) as previously described. Echocardiographic parameter analysis was performed in this study to assess the left ventricular end-systolic diameter (LVESD), left ventricular internal diameter at end-systole (LVIDS), left ventricular end-systolic volume (LVESV), left ventricular end-diastolic volume (LVEDV), left ventricular ejection fraction (LVEF), and left ventricular endocardial fractional shortening (LVEFS). The heart weight (HW) index was defined as the ratio of HW to body weight (BW).

Statistical analysis

Statistical analysis was performed using SPSS 19.0 software for Windows (SPSS Inc, Chicago, Illinois). All data are expressed as the *mean* ± *SD*. Multi-group comparisons were determined by one-way analysis of variance (one-way ANOVA), and the comparison between data from two groups that obey a normal distribution measurement was conducted by t-test. *P*<0.05 was considered significant.

Results

Effects of RTX on ventricular repolarization

The representative electrocardiogram characteristics of each group are shown in **Figure 1A**. The representative APDs recorded from each group are shown in **Figure 1B**. The result shows that compared with the sham group, the ERP and APD90 in MI rats was obviously prolonged, but decreased compared with that of the MI+RTX group (*n* = 3, *P*<0.05) (**Figure 1C**, **1D**). In addition, MI group had prolonged Tend-Tpeak intervals compared with the sham group (**Figure 1E**) (*n* = 3, *P*<0.05), and the Tend-Tpeak interval was shorter in the MI+RTX group than in the MI group (*n* = 3, *P*<0.05).

Effects of RTX on ventricular arrhythmias

Examples of VA in each group are shown in **Figure 2A**. The result shows that the sustained VA was induced in 6 out of 10 MI rats (incidence of 60.31%), and 3 out of 8 RTX+MI rats (incidence of 28.24%); non-sustained VA was

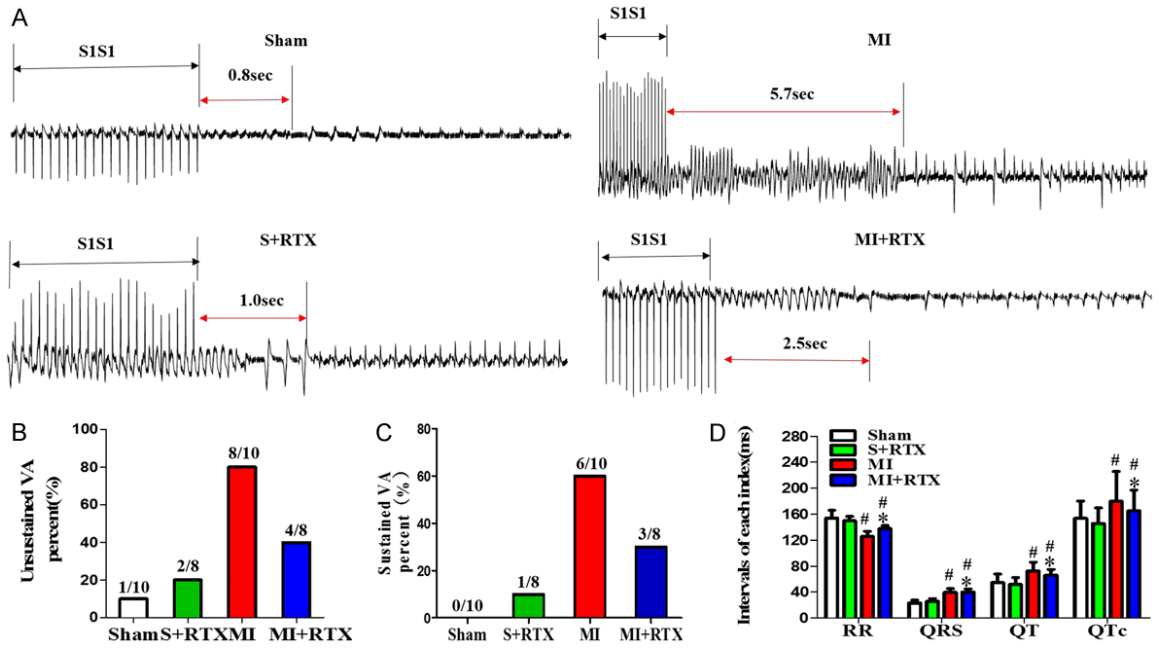

Figure 2. Effects of RTX on ventricular arrhythmias. A. Examples of VA in each group. B. The non-sustained VA percent (%) in each group. C. Sustained VA percent (%) in each group. D. Intervals of each index (ms) (RR, QRS, QT, QTc) in each group. #*P*<0.05 versus sham group; **P*<0.05 versus MI group. VA indicates ventricular arrhythmia.

induced in 8 out of 10 MI rats (incidence of 79.68%), and 4 out of 8 RTX+MI rats (incidence of 41.16%). Analysis of the threshold of the VA incidence indicated that epicardial RTX treatment significantly reduced VA after MI, implying that RTX blocks cardiac afferent nerves and protects against the occurrence and development of VA. In addition, MI prolonged the QRS, QT, and QTc compared with the sham group (**Figure 2D**) (n = 3, P<0.05), and only the QT interval was shorter in the MI+RTX group than in the MI group (n = 3, P<0.05), but there was no statistically significant effect on QRS. In contrast, the RR interval was shortened in the MI group compared with that in the sham group, but prolonged in the MI+RTX group compared with that in the MI group (n = 3, P<0.05). The results suggest that RTX can significantly improve electrophysiological properties.

Effects of RTX on sympathetic nerve remodeling

TH- and GAP43-positive nerve densities were up-regulated in the MI group compared to those in the sham group. The TH- and GAP43-positive nerve densities in the MI+RTX group were less than in the MI group, although the distributions were relatively similar (n = 3, P<0.05) (**Figure 3**). TGF-β1, and cx-43 protein expression were greater in the MI group than in the sham group (n = 3, P<0.05), and they were decreased in the MI+RTX group versus the MI group (n = 3, P<0.05) (**Figure 4**). The results showed that significant sympathetic nerve remodeling can occur during MI, and epicardial RTX injection can significantly improve this phenomenon.

Effects of RTX on serum and tissue norepinephrine (NE) and B-type natriuretic peptide (BNP) levels

As shown in **Figure 5**, NE levels were higher in the MI group compared with the sham group (n = 3, P<0.05), while they were lower in the MI+RTX group than those of the MI group (n = 3, P<0.05), which demonstrated that sympathetic hyperactivity occurred after MI, but it could be reduced by RTX. BNP levels were higher in the MI group compared to the sham group (n = 3, P<0.05), but BNP levels in the MI+RTX group were lower than those in the MI group (n = 3, P<0.05), indicating that RTX can improve BNP levels after MI.

Effects of RTX on cardiac function

Cardiac function in each group is shown in **Table 1** and **Figure 6**. The heart rate and HW/BW ratio in the MI group were significantly high-

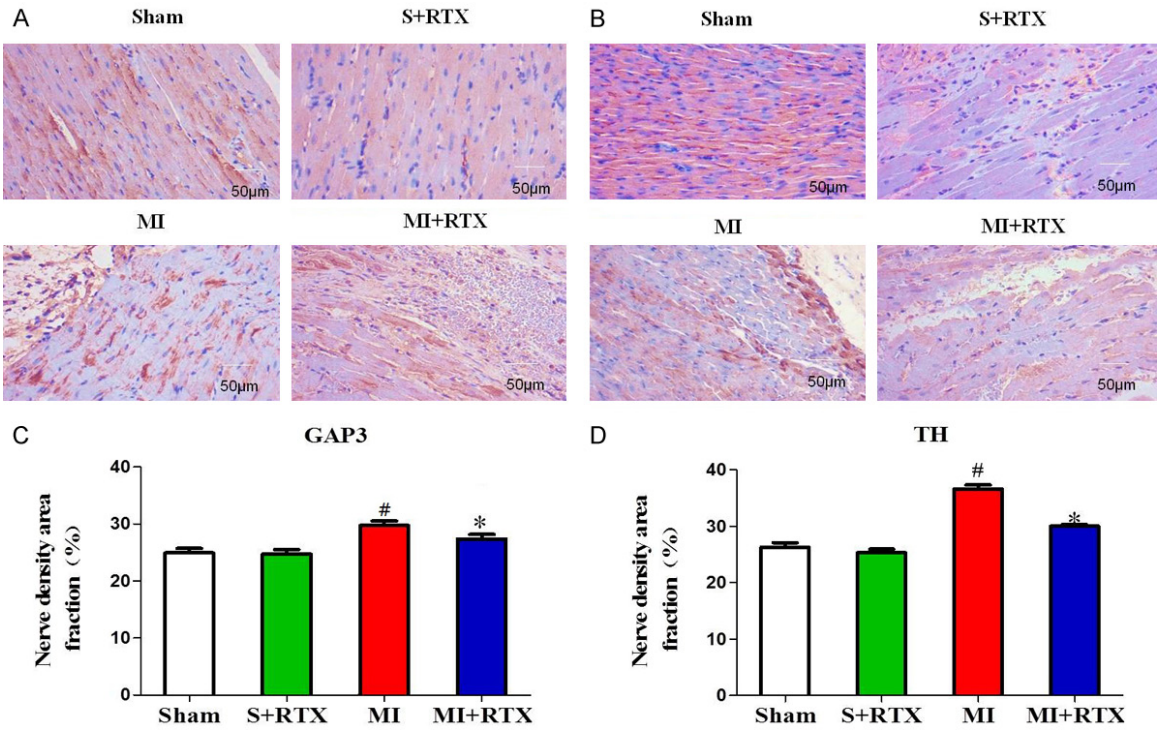

Figure 3. Effect of RTX on distribution of GAP43 and TH. A, B. Representative immunofluorescence of GAP43 and TH by staining with Sirius red dye in four groups.(n = 3). C, D. Relative quantitative analysis GAP43 and TH signals in each group. #P<0.05 versus Sham group. * P<0.05 versus MI group. Magnification, × 200.

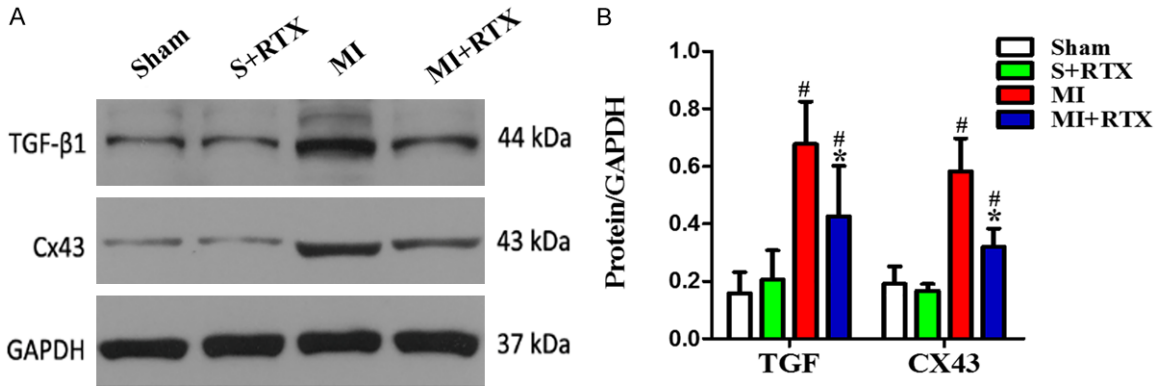

Figure 4. Effect of RTX on TGF-β1, CX43 protein expression. A. Expression of the TGF-β1, CX43 proteins in each group (n = 5). B. Relative quantitative analysis of TGF-β1, CX43 proteins expression. #P<0.05 versus Sham group. *P<0.05 versus MI group.

er than those in the sham group (n = 3, P<0.05), but after epicardial RTX pretreatment, significant decreases in both the heart rate and HW/BW ratio occurred (n = 3, P<0.05), which suggests a protective effect of RTX on cardiac hypertrophy. Compared with sham rats, the MI rats exhibited elevated LVESD and LVESV values (n = 3, P<0.05), and decreased LVEF and LVFS values (n = 3, P<0.05), which indicates decreased ventricular function during MI. After epicardial RTX pretreatment, significant decreases of LVESV and increased LVEF occurred, with LVFS values (n = 3, P<0.05), suggesting that RTX treatment can significantly reduce MI-induced cardiac dilatation, and improve cardiac function.

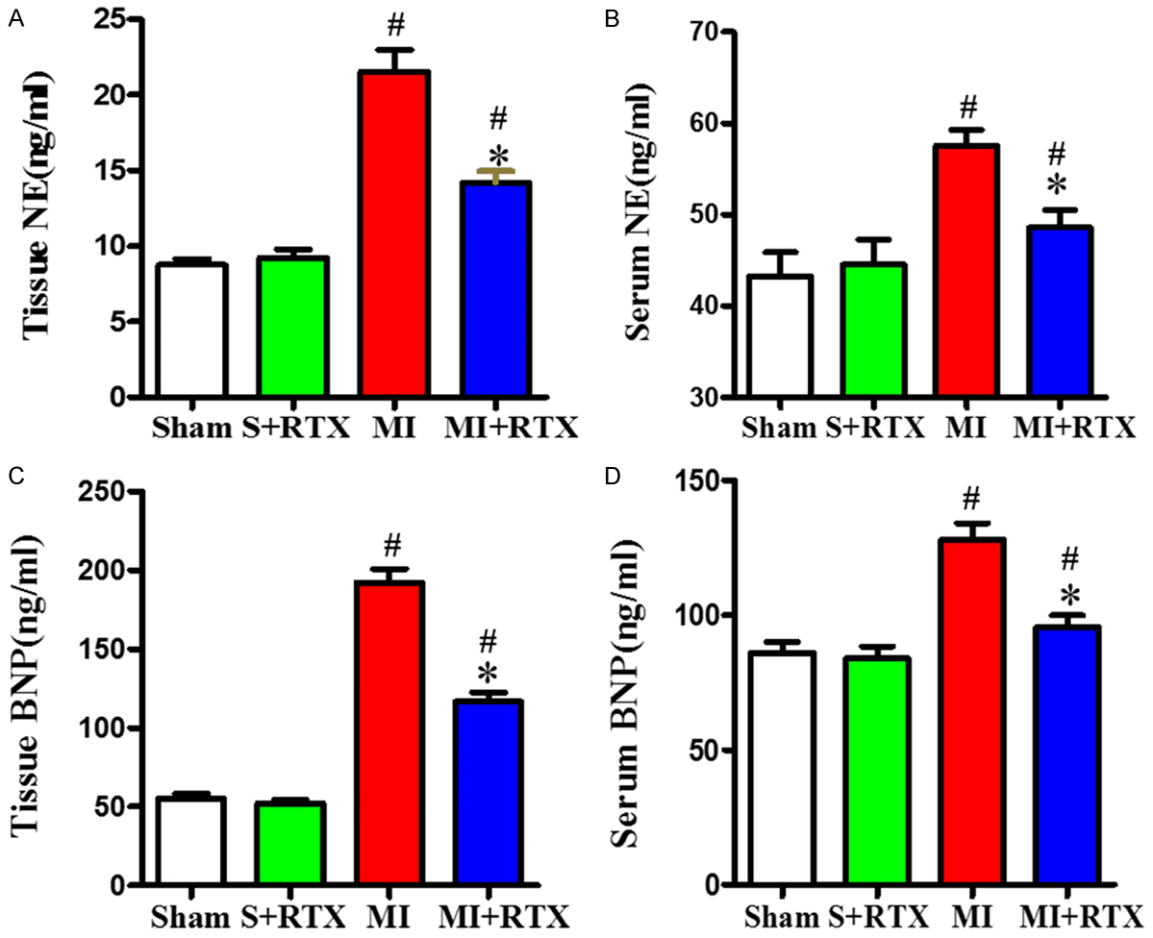

Figure 5. Levels of NE and BNP. A, C. Quantification of tissue NE and BNP levels. B, D. Quantification of serum NE and BNP levels. #P<0.05 versus Sham group. *P<0.05 versus MI group. NE: norepinephrine; BNP: B-type natriuretic peptide.

Table 1. Effect of RTX on cardiac function

Variable	Sham	S+RTX	MI	MI+RTX
Heart rate (bmp)	392.74±45.95	389.93±41.01	484.81±34.41#	434.5±35.08*
Body Weight (g)	421.6±24.47	432.8±12.21	344.8±34.16#	355.6±25.98*
HW/BW ratio (%)	2.67±0.22	2.69±0.12	4.68±0.27#	4.28±0.2*
LVEF (%)	71.35±6.95	71.05±8.98	35.44±5.57#	54.98±7.35*
LVFS (%)	32.73±5.00	38.25±8.94	15.46±4.92#	28.72±6.02*
LVESD (cm)	0.37±0.07	0.38±0.04	0.56±0.07#	0.42±0.08*
LVESV (ml)	0.28±0.05	0.22±0.10	0.43±0.10#	0.30±0.08*

HW: heart weight; BW: body weight; LVESD: left ventricular end-systolic diameter, LVESV: left ventricular end-systolic volume; LVEF: left ventricular ejection fraction; LVFS: left ventricular endocardial fractional shortening; MI: myocardial infarction. #P<0.05 versus Sham group. *P<0.05 versus MI group.

Discussion

Currently, the electrophysiological mechanism underlying the development of significant dispersion of repolarization after MI is not clear. Marked repolarization heterogeneity is caused by adjacent regions of scar tissue, normal myocardium, and hypertrophied myocardium from structural remodeling as previously described [15, 16]. In MI rats, hypertrophied myocardial

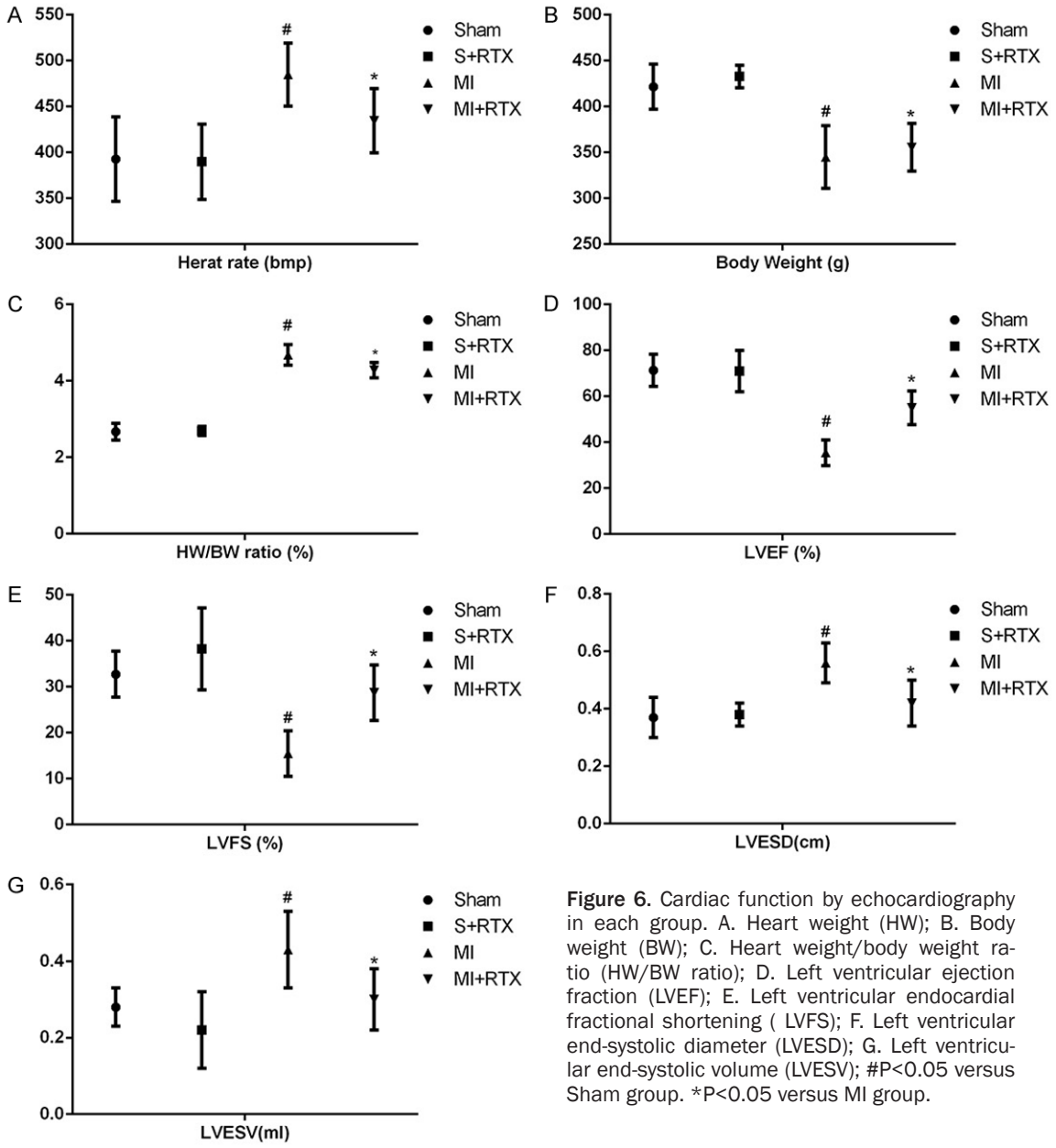

Figure 6. Cardiac function by echocardiography in each group. A. Heart weight (HW); B. Body weight (BW); C. Heart weight/body weight ratio (HW/BW ratio); D. Left ventricular ejection fraction (LVEF); E. Left ventricular endocardial fractional shortening (LVFS); F. Left ventricular end-systolic diameter (LVESD); G. Left ventricular end-systolic volume (LVESV); #P<0.05 versus Sham group. *P<0.05 versus MI group.

tissue or myocardial fibrosis prolongs the action potential duration. Moreover, ERPs and repolarization heterogeneity increased [17]. Regarding cellular electrical remodeling, MI can cause important functional changes in cells, especially border-zone cells, and ion-channel abnormalities mainly through ionic loss, membrane breakdown, and intracellular acidosis [18]. The current study shows that cardiac-induced fibrosis and cardiac electrical remodeling can attenuate electrical interactions between ventricular myocytes and delay transmural activation [19]. Of note, the sympathetic nerve distribution in peri-infarcted areas with sympathetic activity quickly leads to the occurrence of VAs. Additionally, sympathetic stimulation can increase catecholamine secretion and cause cardiac sympathetic nerve redistribution after MI. Myocardial fibrosis and concentric enlargement decreased LV function. Selective denervation of sympathetic afferent nerves with RTX changes the cardiac structure (LV remodeling), enhances LV function, and improves heart failure.

Previous studies have shown that the cardiac sympathetic afferent reflex increases cardiac sympathetic tone and cardiac remodeling in

CHF [20]. RTX can block sympathetic afferent nerves and influence the cardiac neuroendocrine system [21, 22]. A study by Wang *et al* demonstrated that RTX works selectively on local epicardial cardiac sympathetic afferent nerves to cause selective cardiac sympathetic afferent denervation, and reduces cardiac remodeling after MI by interfering with cardiac and renal sympathetic nerves [23]. Nevertheless, our study demonstrated that selective cardiac sympathetic afferent depletion and deafferentation by epicardial RTX treatment prevents excessive local cardiac sympathetic activation in MI rats. The results of our study display that epicardial application of RTX can influence ventricular repolarization, inhibit the occurrence of ventricular arrhythmias, attenuate sympathetic nerve remodeling and sympathetic hyperactivity, and protect cardiac function in rats after MI.

MI elicits the release of various metabolites, that can stimulate cardiac sympathetic afferent nerve endings affecting the ventricular electrophysiological properties (Tend-Tpeak intervals, QRS, QT and so on) [24]. In this study, we found that sympathetic excitation was alleviated by RTX treatment, which prolonged repolarization and reduced the occurrence of VA in MI rats. Interventions targeting cardiac sympathetic activation may be safe and effective strategies to reduce the incidence of lethal VAs. We observed TH- and GAP43-positive cells within the area of MI. Along with gradually increased TH and GAP43, cardiac nerve density was dramatically increased. We also found dramatically increased protein expression levels of TGF-β and cx43 in rats with chronic MI.

Related studies have demonstrated that inhibition of sympathetic excitation prevents myocardial fibrosis in CHF [25]. However, our study found that epicardial RTX treatment significantly reduced MI-induced cardiac dilation and HW/DW index, such as the increase of LV systolic and diastolic diameters and volumes compared with the MI rats, suggesting a protective effect on cardiac muscle.

Conclusions

Epicardial RTX treatment can improve cardiac dysfunction, ventricular electrophysiological properties, and sympathetic nerve remodeling in rats with MI injury.

Acknowledgements

This work was supported by the National Natural Science Foundation of China (No. 81570459).

Disclosure of conflict of interest

None.

Address correspondence to: Congxin Huang, Department of Cardiology, Renmin Hospital of Wuhan University, Cardiovascular Research Institute of Wuhan University, Hubei Key Laboratory of Cardiology, No. 99, Zhangzhidong Road, Wuchang District, Wuhan 430060, Hubei, China. E-mail: huangcongxin1@163.com

References

[1] Kirchberger I, Burkhardt K, Heier M, Thilo C and Meisinger C. Resilience is strongly associated with health-related quality of life but does not buffer work-related stress in employed persons 1 year after acute myocardial infarction. Qual Life Res 2020; 29: 391-401.

[2] Ma S, Ma J, Mai X, Zhao X, Guo L and Zhang M. Danqi soft capsule prevents infarct border zone remodelling and reduces susceptibility to ventricular arrhythmias in post-myocardial infarction rats. J Cell Mol Med 2019; 23: 5454-5465.

[3] Li CY and Li YG. Cardiac sympathetic nerve sprouting and susceptibility to ventricular arrhythmias after myocardial infarction. Cardiol Res Pract 2015; 2015: 698368.

[4] Janse MJ and Wit AL. Electrophysiological mechanisms of ventricular arrhythmias resulting from myocardial ischemia and infarction. Physiol Rev 1989; 69: 1049-1169.

[5] Kettlewell S, Burton FL, Smith GL and Workman AJ. Chronic myocardial infarction promotes atrial action potential alternans, afterdepolarizations, and fibrillation. Cardiovasc Res 2013; 99: 215-224.

[6] Gao H, Yin J, Shi Y, Hu H, Li X, Xue M, Cheng W, Wang Y, Li X, Li Y, Wang Y and Yan S. Targeted P2X7 R shRNA delivery attenuates sympathetic nerve sprouting and ameliorates cardiac dysfunction in rats with myocardial infarction. Cardiovasc Ther 2017; 35.

[7] Hu H, Xuan Y, Wang Y, Xue M, Suo F, Li X, Cheng W, Li X, Yin J, Liu J and Yan S. Targeted NGF siRNA delivery attenuates sympathetic nerve sprouting and deteriorates cardiac dysfunction in rats with myocardial infarction. PLoS One 2014; 9: e95106.

[8] Yin J, Hu H, Li X, Xue M, Cheng W, Wang Y, Xuan Y, Li X, Yang N, Shi Y and Yan S. Inhibition of

Notch signaling pathway attenuates sympathetic hyperinnervation together with the augmentation of M2 macrophages in rats post-myocardial infarction. Am J Physiol Cell Physiol 2016; 310: C41-C53.
[9] Cao JM, Fishbein MC, Han JB, Lai WW, Lai AC, Wu TJ, Czer L, Wolf PL, Denton TA, Shintaku IP, Chen PS and Chen LS. Relationship between regional cardiac hyperinnervation and ventricular arrhythmia. Circulation 2000; 101: 1960-1969.
[10] Szallasi A and Sheta M. Targeting TRPV1 for pain relief: limits, losers and laurels. Expert Opin Investig Drugs 2012; 21: 1351-1369.
[11] Kissin I and Szallasi A. Therapeutic targeting of TRPV1 by resiniferatoxin, from preclinical studies to clinical trials. Curr Top Med Chem 2011; 11: 2159-2170.
[12] Zhang Z, He Y, Tuteja D, Xu D, Timofeyev V, Zhang Q, Glatter KA, Xu Y, Shin HS, Low R and Chiamvimonvat N. Functional roles of Cav1.3 (alpha1D) calcium channels in atria: insights gained from gene-targeted null mutant mice. Circulation 2005; 112: 1936-1944.
[13] Szolcsanyi J, Szallasi A, Szallasi Z, Joo F and Blumberg PM. An ultrapotent neurotoxin of capsaicin-sensitive primary afferent neurons. Ann N Y Acad Sci 1991; 632: 473-475.
[14] Wang X, Xu J, Zhang X, Zhang C, Zheng W, Jiao J, Liu X and Yue X. Effects of Jinlongshe granules on gastric precancerous lesions in rats and its mechanism. Int J Clin Exp Pathol 2020; 13: 846-853.
[15] Gough WB, Mehra R, Restivo M, Zeiler RH and El-Sherif N. Reentrant ventricular arrhythmias in the late myocardial infarction period in the dog. Correlation of activation and refractory maps. Circ Res 1985; 57: 432-442.
[16] Ursell PC, Gardner PI, Albala A, Fenoglio JJ and Wit AL. Structural and electrophysiological changes in the epicardial border zone of canine myocardial infarcts during infarct healing. Circ Res 1985; 56: 436-451.
[17] Qin D, Zhang ZH, Caref EB, Boutjdir M, Jain P and El-Sherif N. Cellular and ionic basis of arrhythmias in postinfarction remodeled ventricular myocardium. Circ Res 1996; 79: 461-473.
[18] Qin M, Liu T, Hu H, Wang T, Yu S and Huang C. Effect of isoprenaline chronic stimulation on APD restitution and ventricular arrhythmogenesis. J Cardiol 2013; 61: 162-168.
[19] Kharin S, Krandycheva V, Tsvetkova A, Strelkova M and Shmakov D. Remodeling of ventricular repolarization in a chronic doxorubicin cardiotoxicity rat model. Fundam Clin Pharmacol 2013; 27: 364-372.
[20] Wang HJ, Rozanski GJ and Zucker IH. Cardiac sympathetic afferent reflex control of cardiac function in normal and chronic heart failure states. J Physiol 2017; 595: 2519-2534.
[21] Dusi V, Zhu C and Ajijola OA. Neuromodulation approaches for cardiac arrhythmias: recent advances. Curr Cardiol Rep 2019; 21: 32.
[22] Wang D, Wu Y, Chen Y, Wang A, Lv K, Kong X, He Y and Hu N. Resiniferatoxin reduces ventricular arrhythmias in heart failure by selectively blunting cardiac sympathetic afferent projection into spinal cord in rats. Eur J Pharmacol 2020; 867: 172836.
[23] Dusi V, Sorg JM, Gornbein J, Gima J, Yanagawa J, Lee JM, Vecerek N, Vaseghi M, Bradfield JS, De Ferrari GM, Shivkumar K and Ajijola OA. Prognostic impact of atrial rhythm and dimension in patients with structural heart disease undergoing cardiac sympathetic denervation for ventricular arrhythmias. Heart Rhythm 2020; 17: 714-720.
[24] Pan HL, Chen SR, Scicli GM and Carretero OA. Cardiac interstitial bradykinin release during ischemia is enhanced by ischemic preconditioning. Am J Physiol Heart Circ Physiol 2000; 279: H116-H121.
[25] Polhemus DJ, Trivedi RK, Gao J, Li Z, Scarborough AL, Goodchild TT, Varner KJ, Xia H, Smart FW, Kapusta DR and Lefer DJ. Renal sympathetic denervation protects the failing heart by inhibition of neprilysin activity in the Kidney. J Am Coll Cardiol 2017; 70: 2139-2153.